



POLITECNICO DI TORINO
Repository ISTITUZIONALE

Analysis of the effects of blast-induced damage zone with attenuating disturbance factor on the ground support interaction

Original

Analysis of the effects of blast-induced damage zone with attenuating disturbance factor on the ground support interaction / Hedayat, A.; Oreste, P.; Spagnoli, G.. - In: GEOMECHANICS AND GEOENGINEERING. - ISSN 1748-6025. - STAMPA. - (2019), pp. 1-11.

Availability:

This version is available at: 11583/2787799 since: 2020-01-31T12:23:17Z

Publisher:

Taylor and Francis Ltd.

Published

DOI:10.1080/17486025.2019.1664777

Terms of use:

openAccess

This article is made available under terms and conditions as specified in the corresponding bibliographic description in the repository

Publisher copyright

(Article begins on next page)

1 **Analysis of the effects of blast-induced damage zone with attenuating disturb-**
2 **ance factor on the ground support interaction**

3 Ahmadreza Hedayat¹, Pierpaolo Oreste², Giovanni Spagnoli³

4 ¹ Assistant Professor, Department of Civil and Environmental Engineering, Colorado School
5 of Mines, 1500 Illinois Street, Golden, CO 80401, USA, hedayat@mines.edu, ORCID: 0000-
6 0002-7143-7272

7 ² Full Professor, Department of Environmental, Land and Infrastructural Engineering, Politec-
8 nico di Torino, Corso Duca Degli Abruzzi 24, 10129 Torino, Italy, pierpaolo.oreste@polito.it,
9 ORCID: 0000-0001-8227-9807

10 ³ Global Project and Technology Manager Underground Construction, BASF Construction
11 Solutions GmbH, Dr.-Albert-Frank-Straße 32, 83308 Trostberg, Germany, [giovanni-](mailto:giovanni.spagnoli@basf.com)
12 ni.spagnoli@basf.com, ORCID: 0000-0002-1866-4345

13 **ABSTRACT**

14 The rock mass properties are typically influenced by the excavation technique and the
15 changes in the state of stress due to the rock excavation. The amount and extent of damage
16 introduced in the rock mass depends on the excavation technique and practice quality. The
17 influence of blasting in the rock mass near the tunnel periphery is far more significant due to
18 the energy of waves and redistribution of stresses and the severity of the damage diminishes
19 as the radial distance from the tunnel opening increases. Therefore, it is important to consid-
20 er the effect of the damaged zone when analyzing the stresses and deformations around a
21 tunnel. This study aimed at providing a new numerical solution for determination of the
22 ground response (reaction) curve with the consideration of the non-uniform damage zone
23 around the tunnel periphery. A deep circular tunnel subjected to hydrostatic stress condition
24 and excavated in rock materials obeying the Hoek-Brown failure criterion is considered. A
25 solution for the determination of stresses, strains, and deformations around the circular deep
26 tunnel is presented in order to **correctly assess the attenuation of damaged rock as the dis-**

27 tance from the tunnel perimeter increases considering the loads applied to the supporting
28 structure.

29 **KEY WORDS:** Disturbance factor; Convergence-confinement method; Damaged zone; Nu-
30 merical solution

31

32

33

34

35

36

37

38

39

40

41

42

43

44

45

46

47

48

49 **ABBREVIATION AND SYMBOLS**

- 50 BIDZ Blast-Induced Damaged Zone;
- 51 CCC Convergence-Confinement Curve;
- 52 CCM Convergence-Confinement Method;
- 53 EDZ Excavation Damage Zone;
- 54 GSI Global Strength Index;
- 55 RQD Rock Quality Designation;
- 56 TBM Tunnel Boring Machines;
- 57 UCS Unconfined Compressive Strength;
- 58 a_p Peak strength parameters of Hoek and Brown;
- 59 D Disturbance factor;
- 60 D_{in} Initial value of the disturbance factor;
- 61 m_i Parameter that depends on the type of intact rock;
- 62 $m_{b,p}$ Peak strength parameters of Hoek and Brown;
- 63 E_{rm} Elastic modulus of the rock mass;
- 64 E_{res} Elastic modulus of the rock mass in residual conditions;
- 65 R Radius of the tunnel;
- 66 R_p Radius of the circular failure zone;
- 67 p_{cr} Critical pressure;
- 68 p_i Internal pressure;
- 69 p_0 Original lithostatic stress in the rock;

70	r	Radius of the damaged zone;
71	$r_{ext,i}$	Distance of the external edge of the i th ring from the tunnel center;
72	$r_{int,i}$	Distance of the internal edge of the i th ring from the tunnel center;
73	s_p	Peak strength parameters of Hoek and Brown;
74	t_{dam}	Thickness of the damaged zone;
75	u	Radial displacement;
76	$u_{ext,i}$	Radial displacement on the external edge of the i th ring;
77	$u_{int,i}$	Radial displacement on the internal edge of the i th ring;
78	ν_{rm}	Poisson coefficient of the rock;
79	ε_r	Radial strain;
80	ε_θ	Circumferential strain;
81	ε_\perp	Perpendicular strain to the plane comprising the radial and circumferential strains;
82	φ_{res}	Residual friction angle of the rock;
83	ψ	Dilatancy angle of the rock;
84	σ_{ci}	Unconfined compressive strength of the intact rock;
85	σ_r	Radial stress;
86	σ_{Rpl}	Radial stress on the plastic radius;
87	$\sigma_{r,ext,i}$	Radial stress on the external edge of the i th ring;
88	$\sigma_{\theta,ext,i}$	Circumferential stress on the external edge of the i th ring;
89	σ_θ	Circumferential stress;
90	σ_\perp	Perpendicular stress to the plane comprising the radial and circumferential stresses.

91 **INTRODUCTION**

92 Any underground excavation or opening is surrounded by zones that have been damaged or
93 disturbed to some extent due to the redistribution of rock stresses that occur upon the crea-
94 tion of an underground excavation or as an effect of the excavation itself (Emsley et al.,
95 1997). Therefore, it is necessary to understand the behavior of the rock mass, and to deter-
96 mine the stresses and displacements around circular openings (Hedayat, 2016). The degree
97 and extent of the Excavation Damage Zone (EDZ) varies significantly based on the selected
98 method of excavation (Read, 1996). In tunnels excavated mechanically by Tunnel Boring
99 Machines (TBM), the effect of the damage in the surrounding rock mass is negligible. In the
100 drill-and-blast (D&B) method, however, the influence of excavation disturbance in the rock
101 mass near the tunnel radius is far more significant (Emsley et al., 1997; Martino and Chan-
102 dler, 2004; Bastante et al., 2012; Zhang et al., 2017).

103 The effect of the damage is evidently greater on the perimeter of the tunnel and tends to de-
104 crease until disappearing at a certain distance from it. For instance, Emsley et al. (1997) and
105 Kwon et al. (2009) stated that only in the near-field (<2 m) the excavation method plays a
106 role causing a damaged zone, with Rock Quality Designation (RQD) values decreasing
107 around 10-15% in comparison with the RQD in undisturbed rock mass (Kwon et al., 2009;
108 Verna et al., 2014).

109 It is, therefore, important to consider the effects of a blast-induced damaged zone (BIDZ)
110 when analyzing the stresses and deformations around an excavation. The development of a
111 BIDZ has a considerable effect on the strength and stiffness of the rock mass. This damage
112 to the material is assumed to form a cylindrical zone of influence at a constant extent (He-
113 dayat et al., 2018). Emsley et al. (1997) discussed the boundary between the damaged (irre-
114 versible changes in rock properties, see Saiang and Nordlund (2009)) and the disturbed (re-
115 coverable changes in rock properties, see Palmström and Singh (2001)), zone is gradational,
116 i.e. there is no distinct boundary but a change which may be defined as the boundary beyond
117 which (at greater distances from the walls) any changes within the rock mass caused by the

118 effects of the excavation are recoverable, thus the disturbed zone, i.e. zone beyond the BIDZ
119 is an elastic region, characterized by undamaged material properties.

120 The assessment of the BIDZ is important and its importance in the design phase varies in
121 different mining, tunneling or petroleum fields (Olsson and Ouchterlony, 2003; Mandal et al.,
122 2005). Daemen (2011) emphasized on the importance of BIDZ assessment in design of nu-
123 clear waste repositories, especially at locations where permanent seals are to be installed
124 and extent and characterization of damaged zone pertaining to design and development of
125 high-level nuclear waste disposal repositories have been extensively studied (Martino and
126 Chandler, 2004; Hudson et al., 2009; Walton et al., 2015). BIDZ in in underground mining
127 and tunneling has, however, received relatively less attention (Scoble et al., 1997). Mandal
128 and Singh (2009) suggested that the damaged zone beyond overbreak zone, i.e. the zone
129 beyond the minimum excavation line of the designed periphery from where rock blocks/slabs
130 detach completely from the rock mass (Verna et al., 2018), should be considered in the de-
131 sign of the tunnel support systems.

132 Interaction between the ground and the support system can be determined by the conver-
133 gence-confinement method (CCM), which describes relationship between the internal applied
134 pressure and the radial displacements of a tunnel wall considering an elasto-plastic analysis
135 of a circular tunnel subjected to hydrostatic far-field stress and uniform internal pressure
136 (Rechsteiner and Lombardi, 1974; Panet, 1995; Peila and Oreste, 1995; Oreste, 2009; 2014;
137 Spagnoli et al., 2016; 2017).

138 Over the years, the convergence-confinement method has also been applied to rock masses
139 with a non-linear failure criterion, as described by Hoek and Brown (1980). When the internal
140 pressure, p_i , in tunnels falls below a critical pressure, p_{cr} , a plastic zone develops around the
141 tunnel (see Fig. 1). When BIDZ is included in the analysis, the dead weight of this broken
142 zone exerts higher pressures to the support system at the crown (roof) of the tunnel which
143 leads to safety factor decrease (e.g. Torbica and Lapčević, 2015; Hedayat et al., 2018). This
144 needs to be considered in the elasto-plastic analysis of the tunnel. However, in order to rep-

145 resent these rock masses in the calculation, some simplifying assumptions are necessary, in
146 particular as far as the strains in the plastic field are concerned (Brown et al., 1983; Carran-
147 za-Torres and Fairhurst, 2000).

148 The current state of practice for the effect of BIDZ is to consider a constant zone of damage
149 for the rock mass with a constant thickness around the tunnel perimeter e.g. Hoek and Kar-
150 zulovic (2000); González-Cao et al. (2018). Obviously, such simplification can lead to errors
151 in the assessment of the convergences that the tunnel can manifest and of the loads that can
152 be applied to the supporting structure. For this reason, in this work the effect of the damage
153 of the rock mass on the static behavior of the tunnel has been investigated, considering a
154 damage that progressively decreases until it disappears at a certain distance from the perim-
155 eter of the tunnel.

156 A numerical solution to the CCM method has been developed in this study, which makes it
157 possible to analyze the behavior of circular openings in rock masses, without the need of
158 introducing any added simplifying assumptions. The utilized approach is the same as that
159 used when a numerical solution is introduced into the CCM (Oreste, 2014). After having pre-
160 sented the formulation necessary to be able to describe the convergence-confinement curve
161 (CCC) of a tunnel excavated in rock masses, some significant results for typical variation
162 intervals of the Disturbance Factor are reported. **The objective of this study is to highlight the
163 importance of certain assumptions about the characteristics of the damaged zone and in par-
164 ticular the need to correctly assess the attenuation of damage to the rock mass as the dis-
165 tance from the perimeter of the tunnel increases.**

166 **THE GEOMECHANICAL PARAMETERS OF THE DAMAGED ZONE**

167 To describe the damage zone, the parameter introduced by Hoek and Brown (2018), called
168 Disturbance Factor (D) is used. This parameter, which varies from 0 to 1 (i.e. 0 in the ab-
169 sence of damage and 1 in case of maximum damage), has the merit of being able to produce
170 an immediate estimate of the geomechanical parameters of the rock mass: not only the pa-
171 rameters of the strength criterion of Hoek and Brown of rock masses (the parameters m_b , s

172 and a) (Hoek and Brown, 2018), but also the elastic modulus E_{rm} (Hoek and Diederichs,
173 2006):

$$174 \quad m_b = m_i \cdot e^{\frac{GSI-100}{28-14D}} \quad (1)$$

$$175 \quad s = e^{\frac{GSI-100}{9-3D}} \quad (2)$$

$$176 \quad a = \frac{1}{2} + \frac{1}{6} \cdot \left(e^{-\frac{GSI}{15}} - e^{-\frac{20}{3}} \right) \quad (3)$$

$$177 \quad E_{rm}(MPa) = 10^5 \cdot \frac{1-D/2}{1+e^{\frac{75+25D-GSI}{11}}} \quad (4)$$

178 where:

179 m_i is a parameter that depends on the type of intact rock (it can be obtained in the laboratory
180 based on the results of triaxial tests);

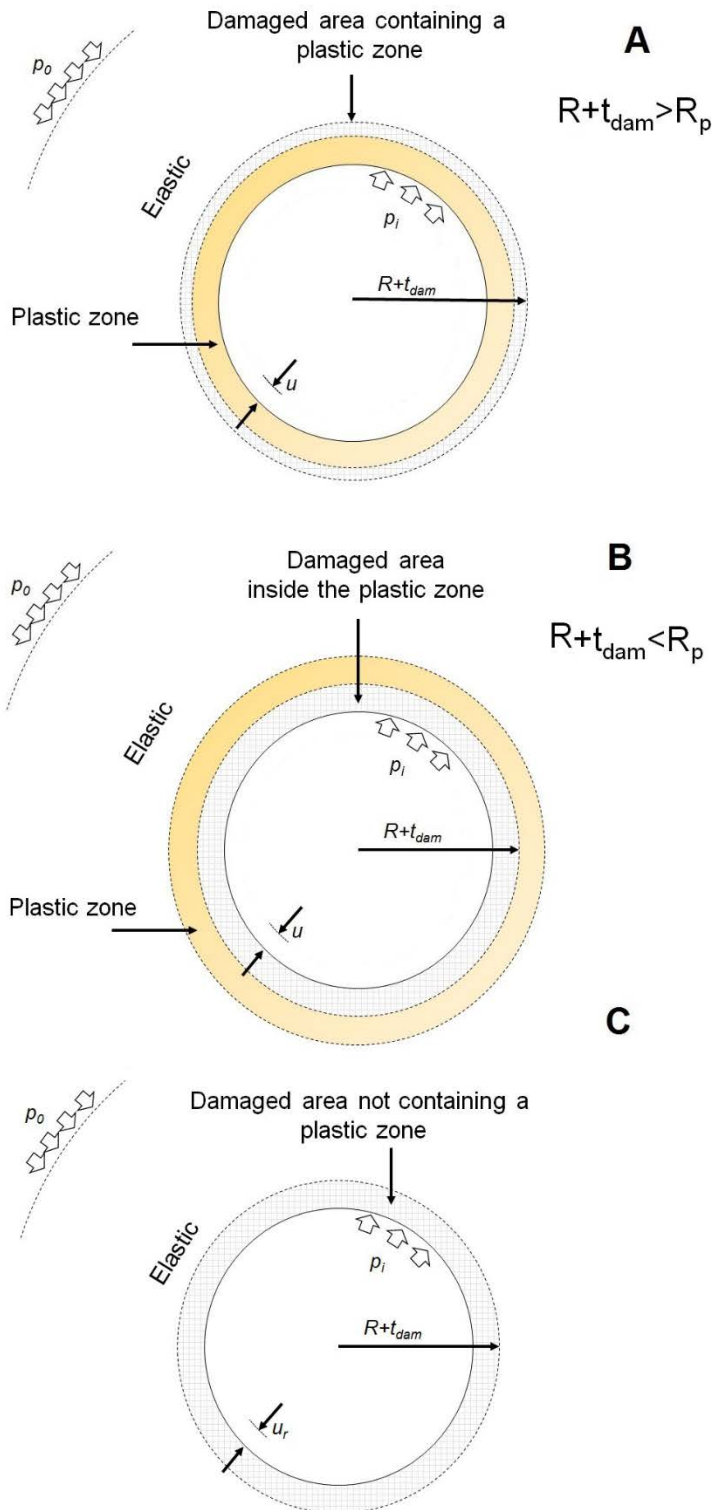
181 GSI is the Global Strength Index (Marinos and Hoek, 2000), which measures the geome-
182 chanical quality of the rock mass;

183 D is the Disturbance Factor.

184 Through **these parameters**, therefore, it is possible to characterize in detail the rock mass in
185 the damaged zone that is present at the edge of the tunnel. More specifically, it is possible to
186 define the geomechanical parameters of the rock mass at each point of the damaged zone,
187 from the perimeter of the tunnel (where the damage is greatest, $D = D_{in}$) to the extreme of
188 the damaged belt where the damage disappears ($D = 0$). For simplicity, a linear trend of the
189 Disturbance Factor was considered within the damaged zone.

190 The tunnel problem considered in this paper is shown in Figure 1. In order to analyze the
191 effects of the presence of the damaged zone on the behavior of the tunnel, the convergence-
192 confinement method of the deep and circular tunnel was used, made of a homogeneous and
193 isotropic material with a hydrostatic stress condition.

194



195

196 **Fig. 1 Sketch of a deep circular tunnel subjected to a hydrostatic stress field with a**
 197 **damaged zone containing a plastic zone (A); with a plastic zone extending beyond the**
 198 **damaged area (B); and with a damaged zone without considering a plastic zone (C).**

199 Because of the blasting impact, a cylindrical BIDZ is developed around the tunnel with differ-
200 ent material properties than the rest of the medium. For this tunnel problem, a uniform sup-
201 port pressure of p_i is assumed to act radially on the interior of the tunnel. As the internal
202 pressure decreases, the tunnel radial convergence u_r increases. The ground reaction curve
203 is by definition the relation between the decreasing internal support pressure and increasing
204 ground convergence. When the radial internal pressure falls below a critical pressure, p_{cr} , a
205 circular failure zone of radius R_p develops around the tunnel. More specifically, the solution
206 proposed by Oreste (2014) was used to determine the convergence-confinement curve of
207 the tunnel excavated in rock masses. This solution:

- 208 1. considers the generalized failure criterion of Hoek-Brown (updated version of 2002)
209 and a law of brittle elasto-plastic behavior;
- 210 2. develops a detailed analysis of plastic deformations in the plastic field;
- 211 3. assumes the dilatation ψ as a percentage value of the residual friction angle φ_{res} of
212 the rock mass, evaluated according to the slope of the strenght criterion on the
213 $\sigma_1 - \sigma_3$ curve
- 214 4. uses a finite difference numerical solution, which provides for the discretization of the
215 plastic zone in 1000 concentric rings.

216 Basically, the rock mass obeys a law of brittle elasto-plastic Hoek-Brown behavior (Hoek et
217 al. 2002). The original solution has been modified and integrated to be able to consider the
218 presence of the damaged zone with the value of the variable parameter D inside it. The
219 changes led to a calculation sequence of this type:

- 220 • evaluation of the fictitious convergence-confinement curves on the external perimeter
221 of the damaged band (at a distance $r = R + t_{dam}$, where R is the radius of the tunnel
222 and t_{dam} is the thickness of the damaged zone), with the determination of several
223 sets of values of the radial and circumferential stresses and of the radial displace-
224 ments ($\sigma_r; \sigma_\theta; u$) for different values of the radial stress σ_r ;

- 225 • division of the damaged zone into 1000 concentric rings in which the stresses and de-
226 formations (as well as the radial displacements) are evaluated starting from the most
227 external ring up to the inner ring next to the tunnel perimeter;
- 228 • determination of the radial stress and of the radial displacement on the inner edge of
229 the last ring next to the tunnel perimeter; this pair of values represents a point of the
230 convergence-confinement curves on the $p - u$ diagram, in the presence of the dama-
231 ged rock area.

232 The numerical solution adopted was suitable to be able to easily deal with the problem of
233 damage variability.

234 **THE CONVERGENCE-CONFINEMENT METHOD APPLICATION IN ROCK MASSESS**

235 The calculation starts from determining the radial stress on the plastic radius (σ_{Rpl}) through
236 the following expression, numerically solved:

$$237 \quad p_0 - p_{cr} = \frac{\sigma_{ci}}{2} \cdot \left(m_{b,p} \cdot \frac{\sigma_{Rpl}}{\sigma_{ci}} + s_p \right)^{a_p} \quad (5)$$

238 The subscript "p" indicates the reference to the peak conditions, different from the residual
239 ones, represented by the "res" subscript throughout the paper, σ_{ci} is the unconfined com-
240 pressive strength (UCS) of the intact rock.

241 For pressures inside the tunnel higher than p_{cr} , the rock mass is entirely elastic and, there-
242 fore, the equations describing the stresses and the strains in the elastic field in the axisym-
243 metric geometry are considered valid. For these pressure values the convergence-
244 confinement curve appears with a linear trend in the internal pressure-radial displacement of
245 the perimeter diagram ($p - u$).

246 For pressures below p_{cr} , a plastic zone around the tunnel appears. In this area, in addition to
247 the strength criterion of Hoek and Brown (in the residual conditions) the following two differ-
248 ential equations are valid:

249 1. The differential equation deriving from the equilibrium of the forces of an infinitesimal
 250 element of rock in the polar coordinates:

$$251 \quad \frac{d\sigma_r}{dr} = \frac{\sigma_\theta - \sigma_r}{r} \quad (6)$$

252 Where σ_θ and σ_r are respectively the circumferential and radial stresses;

253 r is the distance from the tunnel centre.

254 2. The differential equation deriving from the evaluation of strains in the plastic field:

$$255 \quad \frac{du}{dr} = \frac{(1-\nu_{rm}^2)}{E_{res}} \cdot \left[(\sigma_r - p_0) \cdot \left(1 - N_\psi \cdot \frac{\nu}{1-\nu} \right) + (\sigma_\theta - p_0) \cdot \left(N_\psi - \frac{\nu}{1-\nu} \right) \right] - N_\psi \cdot \frac{u}{r} \quad (7)$$

256

257 Where:

258 ν_{rm} is the Poisson coefficient of the rock mass;

259 p_0 is the original lithostatic stress in the rock mass;

260 u is the radial displacement;

261 E_{res} is the elastic modulus of the rock mass in residual conditions;

$$262 \quad N_\psi = \frac{1+\sin\psi}{1-\sin\psi};$$

263 ψ is the dilatancy angle in the rock mass, expressed as a fraction of the residual friction

264 angle.

265 The geomechanical parameters relating to the residual conditions are evaluated by referring

266 to a reduced GSI value:

$$267 \quad GSI_{res} = GSI \quad \text{for } GSI < 35$$

$$268 \quad GSI_{res} = 35 + \frac{1}{2} \cdot (GSI - 35) \quad \text{for } GSI \geq 35$$

269 The friction angle of the rock mass is evaluated in apparent terms, starting from the tangent

270 to the strength criterion, for a given value of the minimum main stress (confinement stress).

271 By varying the pressure inside the tunnel, from the value p_0 to the null value, it is possible to

272 obtain the convergence-confinement curve, i.e. the relation that links the internal pressure to

273 the radial displacement of the tunnel perimeter (Oreste, 2014).

274 **THE VARIABILITY OF THE DISTURBANCE FACTOR IN THE DAMAGED ZONE**

275 Considering the stress and strain state of the damaged zone, it is important to consider the
 276 variation of the Disturbance Factor, D , in the numerical solution. D will be lineary changed
 277 from an initial value, D_{in} , at the edge of the tunnel ($r = R$) until to a null value $D=0$ at the
 278 boundary of the damaged zone. The adopted numerical procedure for finite differences in-
 279 volves starting from the external radius of the damaged zone ($r = R + t_{dam}$), considering one
 280 at a time the 1000 concentric rings of equal thickness in which the damaged zone is divided,
 281 until reaching the last ring next to the perimeter of the tunnel.

282 From the extreme radius of the damaged zone ($r = R + t_{dam}$) the three values ($\sigma_r; \sigma_\theta; u$) are
 283 considered which are obtained from the analysis of the natural rock through the evaluation of
 284 the convergence-confinement curves of the fictitious radius tunnel ($r = R + t_{dam}$). For each
 285 ring considered, it is evaluated whether the stress state is such as to produce the failure of
 286 the rock mass, by checking the achievement of the maximum (major) principal stress value
 287 of the Hoek and Brown strength criterion:

$$288 \quad \sigma_\theta \leq \sigma_r + \sigma_{ci} \cdot \left(m_{b,p} \cdot \frac{\sigma_r}{\sigma_{ci}} + s_p \right)^{a_p} \quad (8)$$

289 where,

290 $m_{b,p}$, s_p and a_p are the peak strength parameters of Hoek and Brown, evaluated in relation to
 291 the value of D attributed to the distance r of the considered ring, being D a linear function of
 292 r .

293 If $\sigma_\theta \leq \sigma_r + \sigma_{ci} \cdot \left(m_{b,p} \cdot \frac{\sigma_r}{\sigma_{ci}} + s_p \right)^{a_p}$ an elastic behavior of the damaged rock is observed,

294 therefore the following equations are valid:

$$295 \quad \varepsilon_r = \frac{(\sigma_r - p_0)}{E_{rm}} - \nu_{rm} \cdot \frac{(\sigma_\theta - p_0)}{E_{rm}} - \nu_{rm} \cdot \frac{(\sigma_\perp - p_0)}{E_{rm}} \quad (9a)$$

$$296 \quad \varepsilon_\theta = \frac{(\sigma_\theta - p_0)}{E_{rm}} - \nu_{rm} \cdot \frac{(\sigma_r - p_0)}{E_{rm}} - \nu_{rm} \cdot \frac{(\sigma_\perp - p_0)}{E_{rm}} \quad (9b)$$

$$297 \quad \varepsilon_\perp = \frac{(\sigma_\perp - p_0)}{E_{rm}} - \nu_{rm} \cdot \frac{(\sigma_r - p_0)}{E_{rm}} - \nu_{rm} \cdot \frac{(\sigma_\theta - p_0)}{E_{rm}} \quad (9c)$$

298 Where:

299 ε_r , ε_θ and ε_\perp are respectively the radial, circumferential and perpendicular (to the plane com-
300 prising the first two) strains;

301 σ_r , σ_θ and σ_\perp are respectively the radial, circumferential and perpendicular (to the plane
302 comprising the first two) stresses;

303 p_0 is the natural lithostatic stress;

304 E_{rm} and ν_{rm} are respectively the elastic modulus and the Poisson coefficient of the rock
305 mass; being E_{rm} function of the Disturbance Factor D , it varies at each ring in relation to the
306 distance r of the ring from the tunnel centre.

307 From the previous equations, being $\varepsilon_\perp=0$ and $\varepsilon_r = du/dr$ we obtain:

$$308 \quad \frac{du}{dr} = \frac{1}{E_{rm}} \cdot [(1 - \nu_{rm}^2) \cdot (\sigma_r - p_0) - (\nu_{rm} + \nu_{rm}^2) \cdot (\sigma_\theta - p_0)] \quad (10)$$

309 Which in numerical terms can be written in the following way for the generic i th ring:

$$310 \quad u_{int,i} = \frac{1}{E_{rm,i}} \cdot [(1 - \nu_{rm}^2) \cdot (\sigma_{r,ext,i} - p_0) - (\nu_{rm} + \nu_{rm}^2) \cdot (\sigma_{\theta,ext,i} - p_0)] \cdot (r_{ext,i} - r_{int,i}) +$$

311 $u_{ext,i}$ (11)

312 where,

313 $u_{ext,i}$ and $u_{int,i}$ are respectively the radial displacements on the external and internal edge of
314 the i th ring;

315 $\sigma_{r,ext,i}$ and $\sigma_{\theta,ext,i}$ are respectively the radial and circumferential stresses on the the external
316 edge of the i th ring;

317 $r_{ext,i}$ and $r_{int,i}$ are respectively the distances of the external and internal edges of the i th ring
318 from the tunnel center. These distances are known, since the damaged zone of thickness
319 t_{dam} was subdivided in 1000 concentric rings of equal thickness ($r_{ext,i} - r_{ext,i} = t_{dam}/1000$).

320 The values of strain and stress on the outer edge of the ring i are the same obtained on the
321 inner edge from the calculation of the previous ring ($i-1$).

322 Furthermore, the following equation of equilibrium of the forces in the radial direction of the
 323 infinitesimal element of rock is always valid (see equation 6). Eq. 6, resolved in numerical
 324 incremental terms, allows to obtain the following equation able to supply the radial stress on
 325 the inner edge of the generic ring i:

$$326 \quad \sigma_{r,int,i} = \sigma_{r,ext,i} - \frac{\sigma_{\theta,ext,i} - \sigma_{r,ext,i}}{(r_{ext,i} + r_{int,i})/2} \cdot (r_{ext,i} - r_{int,i}) \quad (12)$$

327 Because $\varepsilon_{\theta} = u/r$ and by substituting where needed, the incremental numerical equation is
 328 obtained which gives the value of the circumferential stress on the inner edge of the generic
 329 ring i:

$$330 \quad \sigma_{\theta,int,i} = \left[\frac{E_{rm,i} \frac{u_{ext,i} + u_{int,i}}{r_{ext,i} + r_{int,i}} + (v_{rm} + v_{rm}^2) \cdot \left(\frac{\sigma_{r,ext,i} + \sigma_{r,int,i}}{2} - p_0 \right)}{1 - v_{rm}^2} + p_0 \right] \cdot 2 - \sigma_{\theta,ext,i} \quad (13)$$

331 If $\sigma_{\theta} > \sigma_r + \sigma_{ci} \cdot \left(m_{b,p} \cdot \frac{\sigma_r}{\sigma_{ci}} + s_p \right)^{a_p}$ there is a plastic behavior of the damaged rock and, there-
 332 fore, the following equation is valid along with equation 6:

$$333 \quad \sigma_{\theta} = \sigma_r + \sigma_{ci} \cdot \left(m_{b,res} \cdot \frac{\sigma_r}{\sigma_{ci}} + s_{res} \right)^{a_{res}} \quad (14)$$

334 By performing the necessary substitutions, the following incremental numerical formulas are
 335 obtained, capable of evaluating the stress state on the edge inside the generic ring i, once
 336 the stress state on the outer edge is known:

$$337 \quad \sigma_{r,int,i} = \sigma_{r,ext,i} - \frac{\sigma_{ci} \cdot \left(m_{b,res} \cdot \frac{\sigma_{r,ext,i}}{\sigma_{ci}} + s_{res} \right)^{a_{res}}}{r_{ext,i}} \cdot (r_{ext,i} - r_{int,i}) \quad (15)$$

$$338 \quad \sigma_{\theta,int,i} = \sigma_{r,int,i} + \sigma_{ci} \cdot \left(m_{b,res} \cdot \frac{\sigma_{r,int,i}}{\sigma_{ci}} + s_{res} \right)^{a_{res}} \quad (16)$$

339 In the plastic field the displacements are governed by the following differential equation
 340 (Oreste, 2014):

$$341 \quad \frac{du}{dr} = \frac{1 - v_{rm}^2}{E_{res}} \cdot \left[(\sigma_r - p_0) \cdot \left(1 - N_{\psi} \cdot \frac{v_{rm}}{1 - v_{rm}} \right) + (\sigma_{\theta} - p_0) \cdot \left(N_{\psi} - \frac{v_{rm}}{1 - v_{rm}} \right) \right] - N_{\psi} \cdot \frac{u}{r} \quad (17)$$

342 Where $E_{rm,res}$ is the elastic modulus of the rock mass in the residual conditions, calculated
 343 from the GSI in the residual conditions (GSI_{res}). From which the following incremental numer-
 344 ical equation is obtained, which allows to obtain the radial displacement of the inner edge of

345 the generic ring i , once all the other parameters on the outer edge and on the inner edge are
 346 known:

$$\begin{aligned}
 347 \quad u_{int,i} = & \left\{ u_{ext,i} - \frac{(1-\nu_{rm}^2) \cdot (r_{ext,i} - r_{int,i})}{E_{rm}} \cdot \left[\left(\frac{\sigma_{r,ext,i} + \sigma_{r,int,i}}{2} - p_0 \right) \cdot \left(1 - N_\psi \cdot \frac{\nu_{rm}}{1-\nu_{rm}} \right) + \left(\frac{\sigma_{\theta,ext,i} + \sigma_{\theta,int,i}}{2} - \right. \right. \right. \\
 348 \quad & \left. \left. \left. p_0 \right) \cdot \left(N_\psi - \frac{\nu_{rm}}{1-\nu_{rm}} \right) \right] + N_\psi \cdot \frac{u_{ext,i} \cdot (r_{ext,i} - r_{int,i})}{(r_{ext,i} + r_{int,i})} \right\} \cdot \frac{1}{1 - N_\psi \cdot \frac{(r_{ext,i} - r_{int,i})}{(r_{ext,i} + r_{int,i})}} \quad (18)
 \end{aligned}$$

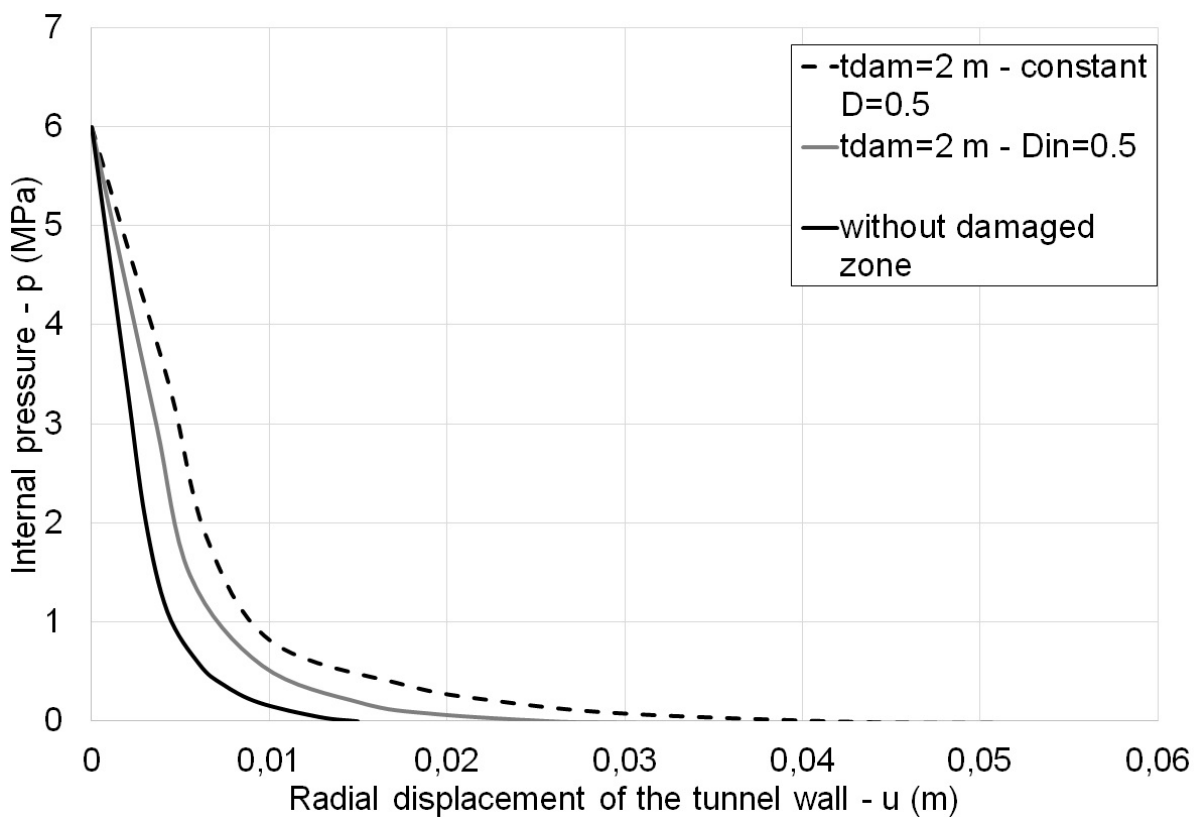
349 Once the last ring is reached, close to the tunnel wall, the values of the radial stress
 350 ($\sigma_{r,int,1000}$) and of the radial displacement ($u_{int,1000}$) on the internal edge represent the pair
 351 of $p - u$ values of the convergence-confinement curve of the tunnel. In this way, at every
 352 point of the fictitious convergence-confinement curve for a radius $r = R + t_{dam}$, corresponds
 353 a point on the real convergence-confinement curves, evaluated considering the presence of
 354 the damaged zone.

355 RESULTS AND DISCUSSION

356 The above calculation procedure has been applied to a specific case, in order to evaluate the
 357 effects of a damaged rock area with variable and decreasing intensity as it moves away from
 358 the tunnel wall. The variation of the Disturbance Factor D was considered linear from an ini-
 359 tial value D_{in} on the perimeter of the tunnel up to a null value at the end of the damaged
 360 zone.

361 The case of a circular tunnel with a radius $R = 3.6$ m, excavated in a rock mass having GSI =
 362 45 (GSI in residual conditions: $GSI_{res} = 40$) has been studied. The lithostatic stress state p_0
 363 was assumed to be 6 MPa, corresponding to a tunnel installed at a depth of about 250 m
 364 from the ground surface. For the intact rock the following characteristic values have been
 365 considered: the uniaxial compressive strength $\sigma_{ci} = 30$ MPa, the m_i parameter of Hoek and
 366 Brown equal to 8. The elastic modulus of the rock mass has been obtained from the equation
 367 of Hoek and Diederichs (2006) both for the peak value (E_{rm}) and residual conditions (E_{res}).
 368 The Poisson ratio of the rock mass (ν_{rm}) was assumed to be constant (i.e. 0.3). The dilatan-
 369 cy angle ψ has been assumed on each point of the plastic zone as 50% of the residual fric-

370 tion angle at that same point. It is therefore variable within the plastic zone in relation to the
 371 stress state (radial stress) variation of the existing at each point with changing distance from
 372 the tunnel centre, r . Initially the calculation was developed assuming the thickness of the
 373 damaged zone of 2 m ($t_{dam} = 2$ m) and a value of the Disturbance Factor on the tunnel wall
 374 equal to 0.5 ($D_{in} = 0.5$) which corresponds to mechanical or hand excavation in poor quality
 375 rock masses (no blasting) resulting in minimal disturbance to the surrounding rock mass
 376 (Hoek, 2007). D varies linearly and decreases progressively as the distance r increases, until
 377 it reaches 0 at the end of the damaged zone ($r = R + t_{dam}$). The result of the convergence-
 378 confinement curves for this hypothesis is reported in Fig. 2, together with two other cases
 379 studied: 1) the absence of the damaged zone; 2) the case of the presence of a damaged
 380 zone of the same thickness ($t_{dam} = 2$ m), but with a constant value of D ($D = 0.5$). This last
 381 case represents the traditional hypothesis that is adopted for simplicity, considering a con-
 382 stant value of the Disturbance Factor within the damaged zone.



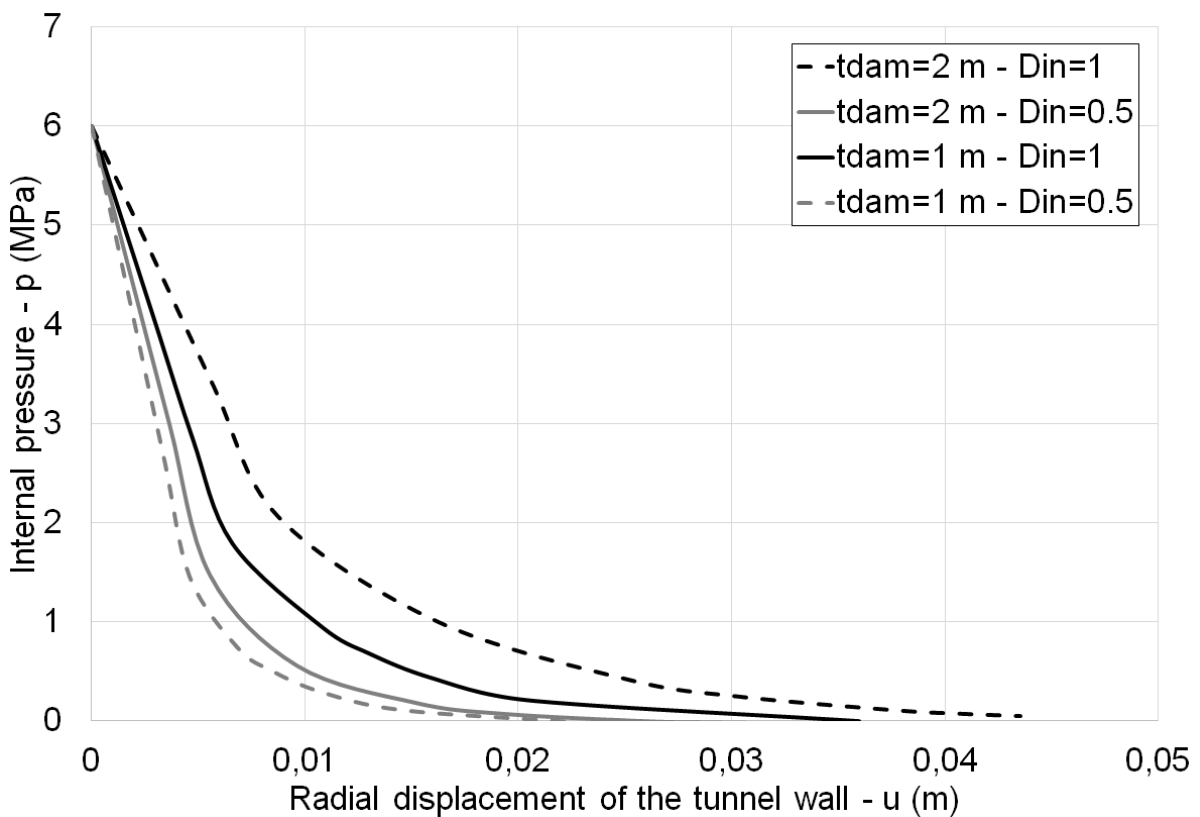
383

384 **Fig. 2 Convergence-confinement curves for the case of the tunnel studied with attenu-**
 385 **ation of the value of the Disturbance Factor in the damaged band (grey line), together**

386 with other two cases: absence of the damaged zone (black line) and presence of a
387 damaged zone with value of D constant (dashed black line).

388 From the analysis of the figure it is possible to see how the effect of the damage on the static
389 behavior of the tunnel is considerably reduced if we consider a linear variation of the Disturbance
390 Factor D (grey line) with respect to the case where D remains constant (simplified ap-
391 proach, dashed black line). On the other hand, the presence of the damaged rock zone can-
392 not be neglected, since there is also a certain difference between the curve obtained from
393 the calculation with the proposed method (grey line) and the case relating to the absence of
394 damaged rock (black line).

395 Then the results of two different values of the thickness of the damaged rock zone ($t_{dam} = 1$
396 and 2 m) and two different initial values of the Disturbance Factor ($D_{in} = 0.5$ and 1) were
397 compared, considering the linear variation of D inside of the damaged zone. The results are
398 shown in the figure 3.



399

400 Fig. 3 Convergence-confinement curves for the 4 analyzed cases, varying the thickness of
401 the damaged zone ($t_{dam} = 1$ and 2 m) and the initial value of D on the tunnel wall ($D_{in} = 0.5$
402 and 1).

403 From the figure 3 it can be noted that the estimation of the maximum value of the damage
404 (D_{in}) on the tunnel wall and the thickness of the damaged zone (t_{dam}) are very important.
405 Both of these parameters strongly influence the trend of convergence- confinement curves,
406 with the relative repercussions on the convergences of the tunnel and, therefore, also on the
407 loads applied to the supporting structures. The intensity of the damage on the perimeter of
408 the tunnel seems, however, to have a more important role than the thickness of the damaged
409 zone.

410 For this reason, great care should be placed on the correct estimation of the factor D at the
411 tunnel wall and also on the thickness of the damaged zone. When it is not possible to obtain
412 these parameters, it is necessary to define a variability interval for them, possibly associating
413 the estimate of this interval with the probability that the real value falls within it. Subsequent-
414 ly, it is possible to proceed with the evaluation of the convergence-confinement curve assum-
415 ing the extreme values of the interval of variability, in order to understand the effect of the
416 limit values of D and t_{dam} on the convergences of the tunnel and on the loads applied to the
417 supporting structures.

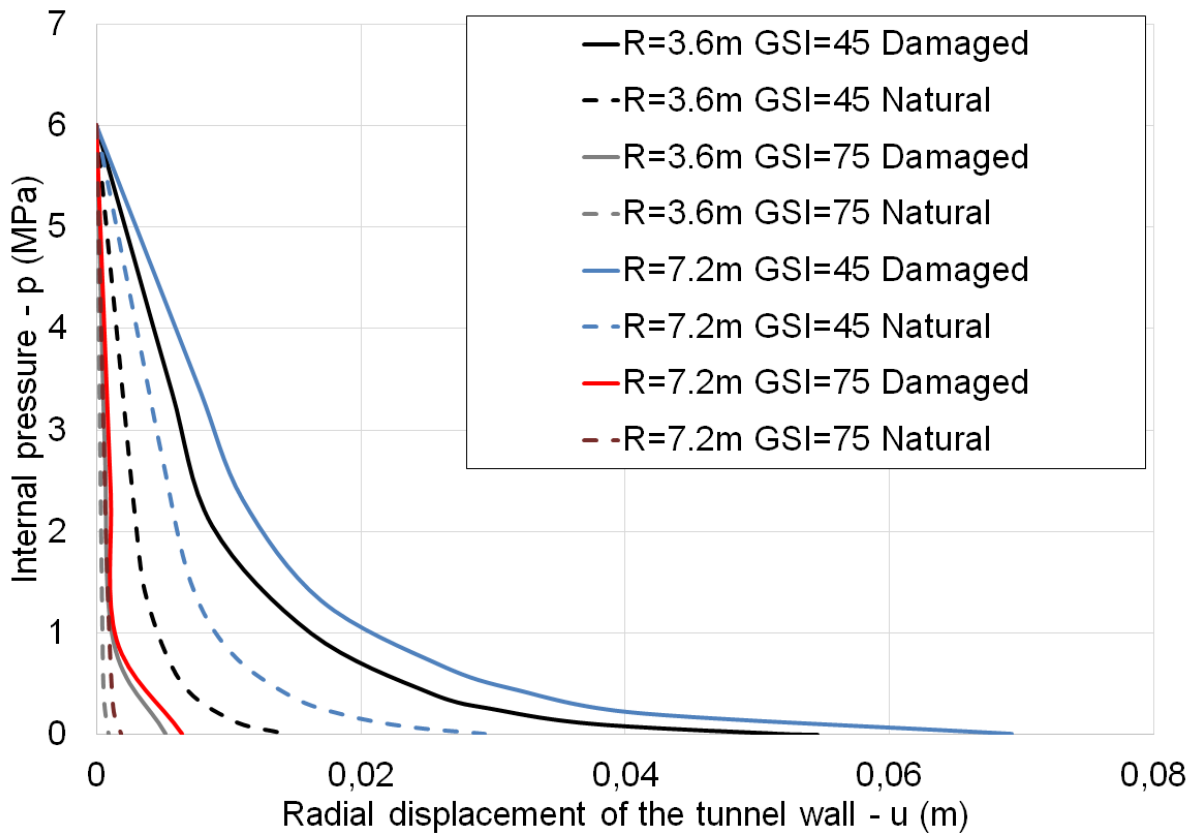
418 Subsequently, in order to study the effect of the damaged rock in terms of pressures and
419 displacements on the perimeter of the excavation, the presence of the same damaged zone
420 around tunnels of different geometry and depth and in the presence of a rock mass was con-
421 sidered with different geomechanical quality.

422 Another 7 cases were analyzed, varying the depth of the tunnel (about 500m with $p_0=12$ MPa,
423 in addition to the case of 250m with $p_0=6$ MPa), its radius R (7.2m in addition to the 3.6m
424 case) and the geomechanical quality of the rock mass (GSI=75, in addition to the case of
425 GSI=45). The case of $p_0 = 6$ MPa, $R = 3.6$ m and GSI = 45 has already been previously dis-
426 cussed.

427 In all cases the presence of a damaged zone of 2m ($t_{dam} = 2m$) and an initial parameter D
428 (D_{in}) on the perimeter of the tunnel equal to 1 was considered. For each of the cases the
429 convergence-confinement curve (CCC) was obtained, which was then compared with the
430 corresponding CCC in natural conditions, i.e. without the presence of the damaged zone.
431 Figs 4 and 5 show the results obtained by the calculation.

432 From the analysis of the figures it can be noted that in the low/medium geomechanical rock
433 masses (GSI=45) the effect of the presence of a damaged area is very important: the charac-
434 teristic curve, considering the presence of the damaged zone, moves upwards in a non-
435 negligible way, both for small/medium-sized and large tunnels. For the tunnels of
436 small/medium size the effect is even greater, considering a damaged area of constant thick-
437 ness in all the cases analyzed. These effects can be found both in shallower tunnels (6MPa)
438 (Figure 4) and in the deeper tunnels (12MPa) (Figure 5).

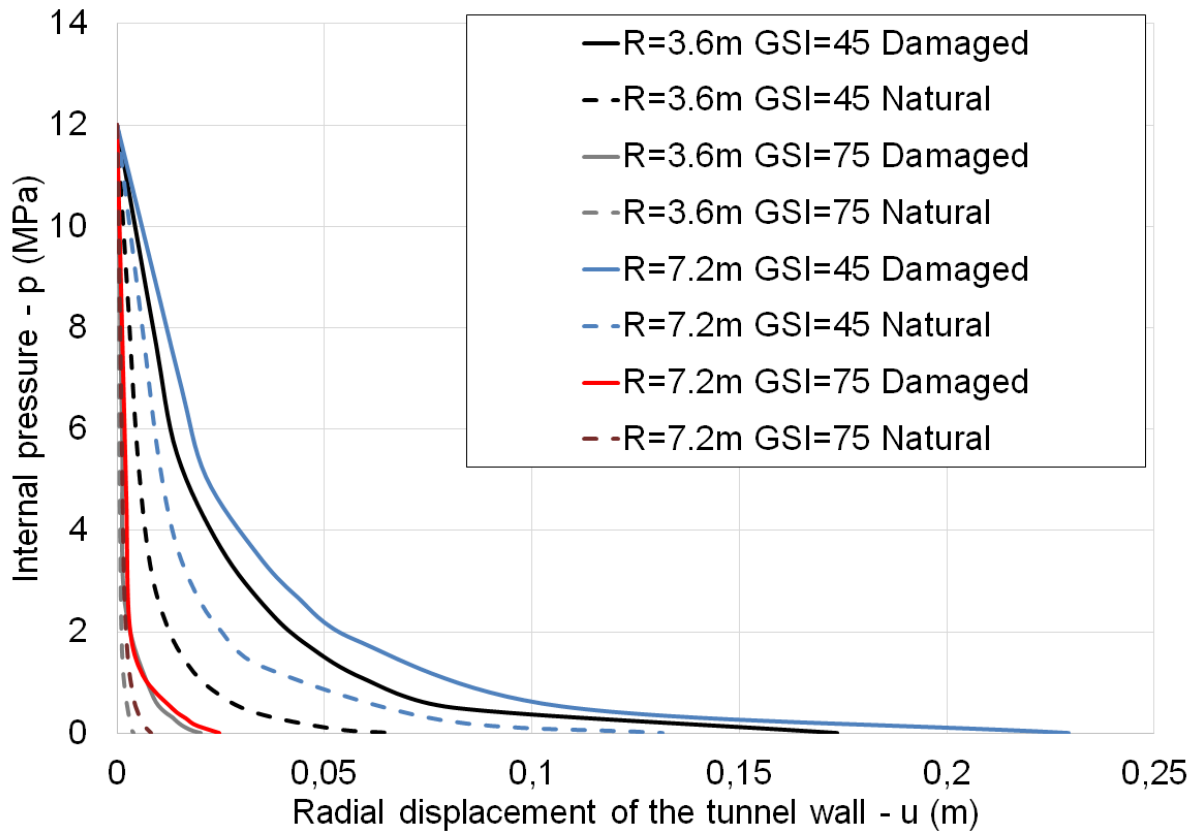
439 Comparison of the CCCs between the damaged and natural conditions reveal that as the
440 damage occurs around the tunnel, for the same amount of internal pressure applied, the
441 convergence is significantly larger. Similarly, for the same level of final convergence using
442 the support system, the required internal pressure and correspondingly the support pressure
443 will be significantly higher for the damage case than the natural case. For this reason, it is
444 very useful to know the effect of the presence of the damaged zone on the CCC, in order to
445 be able to correctly design the supports of the tunnel.



446

447 Fig. 4 Convergence-confinement curves for a tunnel radius of 3.6m and 7.2m ($R = 3.6\text{m}$,
 448 7.2m), a tunnel depth of 250m ($p_0 = 6\text{MPa}$) and GSI index of 45 and 75 (considering the
 449 presence of a damaged zone with $t_{dam} = 2\text{ m}$ and $D_{in} = 1$ and without the presence of a
 450 damaged zone).

451



452

453 Fig. 5 Convergence-confinement curves for a tunnel radius of 3.6m and 7.2m ($R = 3.6\text{m}$,
 454 7.2m), a tunnel depth of 500m ($p_0 = 12\text{MPa}$) and GSI index of 45 and 75 (considering the
 455 presence of a damaged zone with $t_{dam} = 2\text{ m}$ and $D_{in} = 1$ and without the presence of a
 456 damaged zone).

457 CONCLUSIONS

458 In this study, a numerical solution was developed with the consideration of the degree and
 459 extent of the blast induced damage zone around a tunnel. To analyze the effects of the pres-
 460 ence of the damaged zone on the behavior of the tunnel, the convergence-confinement
 461 method of the deep and circular tunnel made of a homogeneous and isotropic material sub-
 462 jected to a hydrostatic stress condition was used. The damage zone with variable D factor
 463 was considered in this study. The presented solution in this paper is novel and allows tunnel
 464 engineers to assess the effect of blasting quality on the ground and support interaction in
 465 tunnels. Several cases were presented to aid with the application of the presented method.
 466 From the example shown previously it was possible to see how the extent to consider the

467 damage area constant for the entire thickness (a simplified approach widely used in practice)
468 can lead to non-negligible errors on the development of the CCC and, therefore, to a consid-
469 erable overestimation of the loads on the supporting structures. The calculation also allowed
470 to note that the estimate of the thickness of the damaged zone and of the initial damage on
471 the wall of the tunnel have a considerable effect on the CCC. This analysis phase needs
472 special care in the design phase of the tunnel.

473 A limited parametric analysis on 8 cases, in which the radius and depth of the tunnel and the
474 geomechanical quality of the rock were changed, allowed to detect how the effect of the
475 presence of a certain damaged area around a tunnel can be especially important in
476 small/medium-sized tunnels in rock masses with low/medium geomechanical properties. The
477 depth, i.e. the original stress state of the rock mass, does not seem to play a fundamental
478 role in influencing the trend of the CCC in the presence of a damaged zone: in fact, the same
479 effects were noted both for the shallower and deeper tunnels.

480 REFERENCES

481 Bastante, F.G., Alejano, L., and Gonzalez-Cao, J. 2012. Predicting the extent of blast-
482 induced damage in rock masses. *International Journal of Rock Mechanics and Mining Sci-*
483 *ences*, 56: 44-53.

484 Brown, E.T., J.W. Bray, B. Ladanyi and E. Hoek, 1983. Ground response curves for rock
485 tunnels. *J. Geotechnical Eng.*, 109: 15-39. DOI: 10.1061/(ASCE)0733-9410(1983)109:1(15).

486 Carranza-Torres, C. and C. Fairhurst, 2000. Application of the convergence-confinement
487 method of tunnel design to rock masses that satisfy the Hoek-Brown failure criterion. *Tunnel-*
488 *ing Underground Space Technol.*, 15: 187-213. DOI: 10.1016/S0886-7798(00)00046-8

489 Daemen, J.J.K., 2011. Nuclear waste disposal in underground mined space, promises –
490 problems/ challenges- solution. *J. Eng. Geol. (India)* 37 (1–4), 37–63.

491 Emsley, S., Olsson, O., Stenberg, L., Alheid, H.J., Falls, S. (1997). ZEDEX - A study of dam-
492 age and disturbance from tunnel excavation by blasting and tunnel boring. Swedish Nuclear
493 Fuel and Waste Management Company, Technical Report, 97-30.

494 González-Cao J, Alejano LR, Alonso E, Bastante, FG (2018). Convergence-confinement
495 curve analysis of excavation stress and strain resulting from blast-induced damage. Tunn
496 Undergr Space Technol. 73:162–169.

497 Hedayat, A. (2016). Stability of circular tunnels excavated in rock masses under gravity load-
498 ing. ARMA-2016-647, 50th U.S. Rock Mechanics/Geomechanics Symposium, 26-29 June,
499 Houston, Texas.

500 Hedayat, A., Weems, J. and Roshan, H. (2018). Stress and deformation analysis of circular
501 tunnels with consideration of blast-induced damage and gravity. ARMA 18–253, 52nd Rock
502 Mechanics/Geomechanics Symposium, 17-20 June, Seattle, Washington.

503 Hoek, E. and E.T. Brown, 1980. Underground Excavations in Rock. 1st Edn., Institution of
504 Mining and Metallurgy, London, pp: 527.

505 Hoek, E. and Karzulovic, A., 2000. Rock mass properties for surface mines. Slope Stability in
506 Surface Mining, (Edited by W.A. Hustralid, M.K. McCarter and D.J.A. van Zyl), Littleton, Colo-
507 rado: Society for Mining, Metallurgical and Exploration (SME), 2000, pp. 59-70.

508 Hoek, E., Carranza-Torres, C., Corkum, B., 2000. Hoek-Brown failure criterion - 2002 Edi-
509 tion. Proc. NARMS-TAC Conference, Toronto, 1, pp. 267-273

510 Hoek, E. and Diederichs, M.S., 2006. Empirical estimation of rock mass modulus. Interna-
511 tional Journal of Rock Mechanics and Mining Sciences, 43, 2, 203-215.

512 Hoek, E., 2007. Practical Rock Engineering.
513 [https://www.rocscience.com/assets/resources/learning/hoek/Practical-Rock-Engineering-Full-](https://www.rocscience.com/assets/resources/learning/hoek/Practical-Rock-Engineering-Full-Text.pdf)
514 [Text.pdf](https://www.rocscience.com/assets/resources/learning/hoek/Practical-Rock-Engineering-Full-Text.pdf)

515 Hoek, E. and E.T. Brown, 2018. The Hoek–Brown failure criterion and GSI – 2018 edition.
516 Journal of Rock Mechanics and Geotechnical Engineering,
517 <https://doi.org/10.1016/j.jrmge.2018.08.001>.

518 Hudson, John A., Backstrom, A., Rutqvist, J., Jing, L., Backers, T., Chijimatsu, M., et al.,
519 2009. Characterising and modelling the excavation damaged zone in crystalline rock in the
520 context of radioactive waste disposal. *Environ. Geol.* 57, 1275–1297.

521 Kwon, S., Lee, C.S., Cho, S.J., Jeon, S.W., Cho, W.J. 2009. An investigation of the excava-
522 tion damaged zone at the KAERI underground research tunnel. *Tunnelling and Underground*
523 *Space Technology*, 24: 1-13.

524 Mandal, S.K., Singh, M.M., Bhagat, N.K., Dasgupta, S., 2005. Causes of overbreak and in-
525 fluence of blast parameters for smooth undamaged wall. In: *Proc. Intl. Sym. On Advances in*
526 *Mining Technology and Management*, November 30–December, 2, IIT, Kharagpur, pp. 49–
527 58.

528 Mandal, S.K., Singh, M.M., 2009. Evaluating extent and causes of overbreak in tunnels.
529 *Tunn. Undergr. Space Technol.* 24, 22–36.

530 Marinos, P. and Hoek, E., 2000. GSI: A Geologically Friendly Tool for Rock Mass Strength
531 Estimation. *Proc. GeoEng 2000 Conference*, Melbourne, pp. 1422-1442.

532 Martino, J.B., Chandler, N.A., 2004. Excavation-induced damage studies at the underground
533 research laboratory. *International Journal of Rock Mechanics and Mining Sciences*, 41,
534 1413–1426.

535 Olsson, M., Ouchterlony, F., 2003. New formula for blast induced damage in the remaining
536 rock, SveBeFo Report No. 65, Swedish Rock Engineering Research, Stockholm.

537 Oreste, P.P., 2007. A numerical approach to the hyperstatic reaction method for the dimen-
538 sioning of tunnel supports. *Tunnelling Underground Space Technol.*, 22: 185-205. DOI:
539 10.1016/j.tust.2006.05.002

540 Oreste P. (2009). "The Convergence-Confinement Method: Roles and limits in modern geo-
541 mechanical tunnel design." *American Journal of Applied Sciences* 6(4), 757-771.

542 Oreste, P. (2014). "A Numerical Approach for Evaluating the Convergence-Confinement
543 Curve of a Rock Tunnel Considering Hoek-Brown Strength Criterion." *American Journal of*
544 *Applied Sciences* 2014, 11(12): 2021-2030.

545 Palmström, A., Singh, R., 2001. The deformation modulus of rock masses – comparisons
546 between in situ tests and indirect estimates. *Tunn. Undergr. Space Technol.* 16 (3), 115–131.

547 Panet, M., 1995. *Le calcul des tunnels par la methode convergence-confinement.* Presses
548 de l'ecole nationale des Ponts et chaussees, Paris.

549 Peila, D. and Oreste, P.P. (1995). "Axisymmetric analysis of ground reinforcing in tunnelling
550 design." *Comput. Geotechnics*, 17, 253-274, DOI: 10.1016/0266-352X(95)93871-F.

551 Rechsteiner, G.F. and G. Lombardi, 1974. Une methode de Calculelasto-Plastique de L'etat
552 de Tension et de Deformation Autourd' unecavitesouterraine. In: *Advances in Rock Me-*
553 *chanics: Proceedings of the 3rd Congress of the International Society for Rock Mechanics,*
554 *National Academy of Sciences, Washington, ISBN-10: 0309022460, pp: 1049-1054.*

555 Read, R.S, 1996. Characterizing excavation damage in highly-stressed granite at AECL's
556 Underground Research Laboratory. In *Proceedings of the Excavation Disturbed Zone Work-*
557 *shop. Canadian Nuclear Society International Conference on Deep Geological Disposal of*
558 *Radioactive Waste, Winnipeg, Canada, 1996.*

559 Saiang, D., Nordlund, E., 2009. Numerical analyses of the influence of blast-induced rock
560 around shallow tunnels in brittle rock. *Rock Mech. Rock Eng.* 42, 421–448. [http://dx.](http://dx.doi.org/10.1007/s00603-008-0013-1)
561 [doi.org/10.1007/s00603-008-0013-1.](http://dx.doi.org/10.1007/s00603-008-0013-1)

562 Scoble, M., Lizotte, Y., Paventi, M., Mohanty, B.B., 1997. Measurement of blast. *Min. Eng. J.*
563 103–108 June, 1997.

564 Spagnoli, G., Oreste, P., and Lo Bianco, L. (2016). New equations for estimating radial loads
565 on deep shaft linings in weak rocks. *Int. J. Geomech*, 16(6): 06016006, DOI:
566 [10.1061/\(ASCE\)GM.1943-5622.0000657](https://doi.org/10.1061/(ASCE)GM.1943-5622.0000657).

567 Spagnoli, G, Oreste, P, and Lo Bianco, L. (2017). Estimation of Shaft Radial Displacement
568 beyond the Excavation Bottom before Installation of Permanent Lining in Nondilatant Weak
569 Rocks with a Novel Formulation. *Int. J. Geomechanics*, 17(9), 04017051
570 [https://doi.org/10.1061/\(ASCE\)GM.1943-5622.0000949](https://doi.org/10.1061/(ASCE)GM.1943-5622.0000949).

571 Torbica, Z. and Lapčević, V. (2015). Estimating extent and properties of blast-damaged zone
572 around underground excavations. *Rem: Revista Escola de Minas*, 68(4), 441-453.

573 Verna, H.K., Samadhiya, N.K., Singh, M. and Prasad, V.V.R. (2014). Blast induced damage
574 to surrounding rock mass in an underground excavation. *Journal of Geological Resource and*
575 *Engineering* 2, 13-19.

576 Verna, H.K., Samadhiya, N.K., Singh, M., Goel, R.K. and Singh, P.K. (2018). Blast induced
577 rock mass damage around tunnels. *Tunnelling and Underground Space Technology* 71,
578 149–158.

579 Walton, G., Latob, M., Anschütz, H., Perrard, M.A., Diederichse, M.S., 2015. Non-invasive
580 detection of fractures, fracture zones, and rock damage in a hard rock excavation – Experi-
581 ence from the Äspö Hard Rock Laboratory in Sweden, *Eng. Geol.* 28 Sep vol. 196, pp. 210–
582 221.

583 Zhang, Y., Lu, W., Yan, P., Chen, M., Yang, J. 2017. A method to identify Blasting-Induced
584 Damage Zones in rock masses based on the P-wave rise time. *Geotechnical Testing Jour-*
585 *nal*, 41(1): 31-42.